Algal Research 80 (2024) 103548

Contents lists available at ScienceDirect

Algal Research

journal homepage: www.elsevier.com/locate/algal

# Insights into the structuring ability of two brown seaweeds (*Laminaria digitata* and *Saccharina latissima*) for applications as natural texturisers

Antonio Souto-Prieto [a], Marta Martinez-Sanz [b], Tania Ferreiro [c], Patricia Parada-Pena [c], Laura Abuin-Arias [c], Angel Cobos [a], Patricia Lopez-Sanchez [a,c,d,*]

[a] Department of Analytical Chemistry, Nutrition and Food Science, Facultad de Ciencias, Universidade de Santiago de Compostela, Campus Terra, Lugo 27002, Spain
[b] Instituto de Investigación en Ciencias de la Alimentación, CIAL (CSIC-UAM, CEI-UAM + CSIC), Nicolás Cabrera 9, Madrid 28049, Spain
[c] Dairy Products and Food Technology Centre APLTA, Universidade de Santiago de Compostela, Campus Terra, Rua Montiron, Lugo 27002, Spain
[d] Instituto de materiales (iMATUS), Universidade de Santiago de Compostela, Avenida do Mestre Mateo 25, Santiago de Compostela 15706, Spain

ARTICLE INFO

*Keywords:*
Seaweed
Rheology
High pressure homogenisation
Structure
Cell wall
SAXS

ABSTRACT

Seaweeds represent a potential source of new food products with enhanced sustainability. However, in order to use seaweeds as ingredients more knowledge is needed regarding the impact of processing on their structuring ability and functionality. We report on the structure and rheology of aqueous dispersions of two species of brown seaweed, namely: *Laminaria digitata* and *Saccharina latissima*, prepared by different food processing techniques. High pressure homogenisation disrupted seaweed cell walls, leading to stable weak gels characterised by smaller particle size compared to untreated samples. Thermal treatment (70 °C 1 h), applied prior or during shear treatment, did not impact the particle size, however, it led to serum phases with higher viscosities. This was related to an increased solubilisation of polysaccharides from the cell walls into the serum, as reflected by chemical analysis and small angle X-ray scattering (SAXS). Furthermore, although in terms of rheological behaviour and particle size, both species showed similar response to food processing conditions, the cell wall nanostructure of *L. digitata* was modified to a larger extent compared to *S. latissima*, which was linked to a higher solubilisation of polysaccharides. These insights regarding functionalisation of brown seaweed dispersions provide the scientific knowledge to use whole seaweed as natural structurants for future food and other technological applications.

## 1. Introduction

Exploring new food sources is required to create a more sustainable and resilient food system, within the current societal challenges associated to food security. Among the new food sources, marine macroalgae have emerged as an alternative source rich in bioactive compounds, including polysaccharides, proteins, and minerals [1]. Seaweeds may offer not only unique nutritional profiles, alternative flavours, and dietary diversity but also contribute to human health [2,3]. Regarding alternative proteins, seaweeds have gained particular interest and, current investigations focus on extraction processes and digestibility of protein from different species [4]. In the case of brown seaweed, protein content and extraction yields are low compared to other species [5]. This is due to the recalcitrant nature of their cell walls and, also the interactions taking place between proteins and other seaweed components such, as polysaccharides and polyphenols [6].

Therefore, brown seaweed have the potential to be used as a whole ingredient, rather than as a source of protein extracts. From a biological point of view, phylogenetic studies indicate that the cell walls of brown seaweed have evolved independently of other algae and land plants [7]. Brown seaweed cell wall possess a unique polysaccharide composition, primarily consisting of alginate, laminarin, and fucoidan [6] and a low content (approximately 10 % dry weight) of cellulose [8]. In particular, alginate extracted from brown seaweeds is widely used in food and pharmaceutical industry as a gelling agent [9,10]. However, the integration of brown seaweed as a whole ingredient into mainstream diets is hindered by challenges related to texture, taste, and limited knowledge regarding nutrients bioaccessibility.

To address these challenges, innovative processing technologies are being explored to retain the nutritional value of seaweeds [11], as well

* Corresponding author at: Department of Analytical Chemistry, Nutrition and Food Science, Facultad de Ciencias, Universidade de Santiago de Compostela, Campus Terra, Lugo 27002, Spain.
*E-mail address:* patricialopez.sanchez@usc.es (P. Lopez-Sanchez).

https://doi.org/10.1016/j.algal.2024.103548
Received 8 February 2024; Received in revised form 29 April 2024; Accepted 12 May 2024
Available online 17 May 2024

as to investigate their impact on flavour [12,13] and textural properties [14,15]. A possible route to optimise the techno and bio-functional properties of seaweeds is to modify their cell wall structure and physical properties by thermal and/or non- thermal food processes, which disrupt cell wall structures by modifying and solubilising wall components. High pressure homogenisation (HPH), a mechanical process involving the application of high pressures and shear forces, has been successfully employed to disrupt cellular structures, modifying rheological properties of vegetables [16] and microalgae dispersions [17]. Our own research [18] has shown that HPH modified the microstructure and rheological properties of dispersions of the brown seaweed *Laminaria digitata*; however, the impact on the cell wall nanostructure and optimisation of high shear conditions remained elusive. Cell wall nanostructures are relevant from a food science and nutrition perspective as they are the barrier that enzymes and micronutrients have to overcome to reach the substrates and absorption sites, respectively. Thus, modification on cell wall nanostructures during processing could have a positive impact on bioaccessibility.

Seaweed dispersions typically consist of insoluble particles dispersed in a liquid continuous phase. Thermal and non-thermal processing of these dispersions may lead to changes in the nature of the particles *i.e* size, shape, surface charge and composition, and in the interactions and arrangement of the dispersed components, along with the continuous phase. Such changes affect their ability to flow and deform under applied stresses giving rise to their rheological properties. Understanding and controlling these structural and rheological parameters is highly relevant in designing food formulations with the desirable texture, stability, and sensory attributes.

In this work, we investigated the impact of the combination of thermal and mechanical food processing techniques, on the micro and nanostructure of aqueous dispersions of two brown seaweed species, *Laminaria digitata* and *Saccharina latissima*. Flow behaviour and viscoelasticity, characterised by small amplitude oscillatory shear measurements, were evaluated and related to particle size distribution and solubility of cell wall polysaccharides. Furthermore, small angle X-ray scattering (SAXS) was applied for the first time to investigate seaweed cell walls, rather than individual cell wall components, to elucidate the impact of processing on the nanostructure of cell walls. The findings from this research could contribute to the development of innovative seaweed-based products with improved texture, functionality, and nutritional benefits.

## 2. Materials and methods

### 2.1. Raw materials

Brown seaweed *Laminaria digitata* (LD) and *Saccharina latissima* (SL) were acquired from a seaweed grower (KosterAlg, Sweden). Seaweeds were grown and dried following food grade conditions. Seaweed powders were prepared by first blending the seaweed blades in a food processor (Thermomix TM6, Vorwerk, Germany) for 30 s, followed by grinding (Super junior "S", Moulinex, France) for 30 s. The obtained materials were sieved (Cisa, Barcelona, Spain) to standardise their particle size. The fraction with the highest yield consisted of particles between 125 and 425 μm, therefore this fraction was utilised in this study.

### 2.2. Sample preparation

Seaweed dispersions (5 % *w/v*) were prepared by mixing seaweed powder with water and allowing it to rehydrate overnight at 5 °C. Each sample was divided into 3 batches of 1 kg. Two of the batches were thermally treated at 70 °C for 1 h in a Thermomix (TM6, Vorwerk, Germany). All samples underwent a mechanical treatment in an Omni Mixer (Homogeniser, Silverson, East Longmeadow, USA) at maximum speed (approximately 18,000 rpm) for 3 min followed by high pressure homogenisation HPH (APV Lab 2000, SPXFlow, Mecklenburg, USA) either at room temperature or at 70 °C. In the high pressure homogeniser, the samples were processed using two-stage homogenisation and 3 cycles with the following whole pressure (P1) to back pressure (P2), ratio P1/P2: in cycle 1 the ratio was 15/1 MPa, in cycle 2 and 3 were 50/5 MPa. Samples codes are described below:

- LD HPH: *Laminaria digitata*. No thermal treatment, HPH at room temperature.
- LD 70 °C HPH: *Laminaria digitata*. Thermal treatment 70 °C for 1 h + HPH at room temperature.
- LD 70 °C HPH 70 °C: *Laminaria digitata*. Thermal treatment 70 °C for 1 h + HPH at 70 °C.
- SL HPH: *Saccharina latissima*. No thermal treatment, HPH at room temperature.
- SL 70 °C HPH: *Saccharina latissima*. Thermal treatment 70 °C for 1 h + HPH at room temperature.
- SL 70 °C HPH 70 °C: *Saccharina latissima*. Thermal treatment 70 °C for 1 h + HPH at 70 °C.

Samples were taken before and after each proccessing step. Samples were vacuum packed in polyethylene bags after adding 100 μL of 0.02 % sodium azide ($NaN_3$) to prevent microbial growth during storage prior to analysis. Processing conditions are summarised in Fig. 1. The serum phase (supernatant) and the dispersed phase (pellet) of the dispersions before and after treatment were separated by centrifugation (Digicen 21R, Orto Alresa, Spain) at 4600 g for 15 min at 25 °C. Part of the serum was used for viscosity measurements and SAXS, the remaining amount was freeze-dried for subsequent monosaccharide analysis.

### 2.3. Chemical composition

Dry matter: Seaweed powders were measured using a moisture analyser (Dab 100-3, Kern & Sohn, Ebingen, Germany). For the thermogravimetric analysis, 8 g of sample were weighed and evenly distributed on a plate and dried at 100 °C using a standard heating profile. For the dispersions and sera, the solid content was measured by drying in an oven at 115 °C for 12 h. Samples were measured in duplicates.

Protein content: The determination of the total protein was performed by the Kjeldahl method [19]. Samples (1 g) were weighed and measured in duplicates. A nitrogen protein factor of 5.6 was used to calculate the total protein content for seaweed [20].

Fat content: For the determination of total fat, the Röse-Gottlieb method was used [21] adapted to seaweed. Samples were weighed (0.6 g) and the fat extraction was carried out with petroleum ether or diethyl ether a total of three times. Once the fat was collected, samples were dried in a oven at 100 °C for 1 h. They were introduced into a desiccator

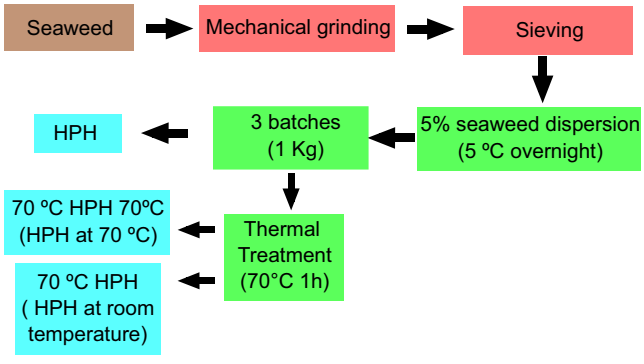


**Fig. 1.** Schematic overview of the processing of brown seaweed dispersions. HPH = high pressure homogenisation. (For interpretation of the references to colour in this figure legend, the reader is referred to the web version of this article.)

to cool down and weighed.

Ash content: Ash was measured as the difference in weight between the sample before and after drying in a muffle furnace at 550 °C for 3 h [22].

Total phenols: the phenol content was measured by the Folin-Ciocalteu method applied to seaweed [23]. Gallic acid solutions were prepared in water with concentrations of 100, 80, 60, 40, 20, 10, 5 and 1 mg/L as calibration standards. For the preparation of the seaweed samples (duplicates), 0.5 g was weighed and mixed with 50 mL of 80 % methanol [24], ultrasonicated and centrifuged at 4600 ×*g* for 12 min. 1 mL of sample (or standard solution) was mixed with 9 mL of deionised water and 1 mL of the Folin-Ciocalteu reagent and, the mixture was left to stand for 5 min. Once the time had elapsed, 10 mL of $Na_2CO_3$ (7 % *w/v*) was added and the volume was adjusted to 25 mL with deionised water. The mixtures were left to stand at room temperature for 90 min [24]. The absorbance of the samples was measured at 750 nm (V630 Spectrophotometer, Jasco, Tokyo, Japan).

### 2.4. Calcium analysis by inductively coupled plasma (ICP-MS)

Seaweed powders were subjected to microwave assisted extraction in combination with acid digestion. In brief, the powders were mixed with 2 mL of MilliQ water and 3 mL of nitric acid (70 % *w*/w). Samples were microwaved (ultraWAVE microwave laboratory station, Milestona, Sorisole, Italy) three times, one sample blank was also prepared. Microwave irradiation consisted of a time ramp of 40 min to increase the temperature from 20 to 260 °C at 1500 W and 4 MPa. The digested sample was brought to a final volume of 10 mL with MilliQ water. Calcium was determined in an inductively coupled plasma mass spectrometer (Agilent 7900, Agilent Technologies, California, United States). Measurements were performed in triplicate.

### 2.5. Monosaccharides analysis

The monosaccharide composition of the seaweed powders, the dispersions and the supernatants separated after centrifugation was determined after two-step methanolysis [18]. 1 mg of dry sample was hydrolysed using 1 mL of 2 M HCl in dry methanol at 100 °C for 5 h. Samples were then neutralised with pyridine and dried under nitrogen flow. Hydrolysis was carried out using 2 M trifluoro acetic acid (TFA) at 120 °C for 1 h in an autoclave [25]. Samples were dried again under air, resuspended in water and filtered through 0.2 μm nylon filter (Branchia, Labbox, España) before injection onto a ionic cromatographer with pulsed amperometric detection system (Metrohm 930 IC Flex, Metrohm Hispania, Madrid, Spain) equipped with a Metrosep Carb 2 column (4 × 250 mm, Metrohm). The temperature of the column was 30 °C, injection volume was 20 μL and flow rate 0.6 mL/min. The eluent program was applied as described by [18]. Neutral and uronic sugar standards at concentrations between 1 and 25 mg/L were used for the quantification of monosaccharides.

### 2.6. Particle size measurements

The particle size distribution was measured by light scattering in a Mastersizer (Hydro 2000SM, Malvern Instruments, Worcestershire, UK). Approximately 0.5 mL of aqueous dispersion of seaweed were added into a small sample volume dispersion unit (Malvern Instruments, Worcestershire, United Kingdom) filled with deionised water under continuous agitation (3000 rpm). For the measurement of the particle size, the software was configured with a refractive index of 1.47 and an absorption of 0.01 [18]. The model applied was the "general purpose" with a normal sensitivity. Due to the irregularity in the shape of the particles, the "irregular shape" option was chosen. An obscuration between 5 % and 10 % was selected for all measurements, which were performed in triplicate. The particle size distribution was calculated by the instrument software (Mastersizer 2000, Malvern Instruments, Worcestershire, UK) from the dispersed light intensity profile. In highly polydisperse systems, such as these seaweed dispersions, the surface base diameter $D_{[3,2]}$ is selected as the indicator of the average particle size [16].

### 2.7. Confocal laser scanning microscopy (CLSM)

Confocal laser scanning microscopy was used to observe the morphology of the seaweed particles. Samples were placed on a glass slide and covered by a cover glass. Imaging was performed using a Leica TCS SPE confocal system (Leica Microsystems GmbH, Wetzlar, Germany). The microstructure was studied using a ×20 air objective lense. A solid-state laser emitting at 488 nm was used for excitation. Autofluorescence from chlorophyll was detected in the range from 645 to 715 nm.

### 2.8. Small angle X-ray scattering (SAXS)

SAXS experiments were carried out in the Non Crystalline Diffraction beamline, BL-11, at ALBA synchrotron light source [26]. The seaweeds powders and the aqueous dispersions obtained after the thermal and mechanical treatments, as well as their respective serum phases, were placed into sealed 2 mm quartz capillaries (Hilgenberg GmbH, Germany) and analysed. The energy of the incident photons was 12.4 keV or equivalently a wavelength, $\lambda$, of 1. The SAXS scattering patterns were collected by means of a photon counting detector, Pilatus 1 M, with an active area of 168.7 × 179.4 $mm^2$, an effective pixel size of 172 × 172 $\mu m^2$ and a dynamic range of 20 bits.

The sample-to-detector distance was set to 6530 mm, resulting in a q range with a maximum value of q = 0.2 $Å^{-1}$. An exposure time of 10 s was selected based on preliminary trials. The data reduction was treated by pyFAI python code (ESRF) [27], modified by ALBA beamline staff, to do on-line azimuthal integration's from a previously calibrated file. The calibration files were created from a silver behenate (AgBh) standard. The intensity profiles were then represented as a function of q using the IRENA macro suite [28] within the Igor software package (Wavemetrics, Lake Oswego, Oregon). The scattering patterns from the serum samples were properly described using a unified model:

$$I(q) = \sum_{i=1}^{N} G_i exp\left(-q^2 \cdot \frac{R_{g,1}^2}{3}\right) + \frac{B_i\left[erf\left(qR_{g,1}/\sqrt{6}\right)\right]^{3P_i}}{q^{P_i}} + bkg \quad (1)$$

This model considers that, for each individual level, the scattering intensity is the sum of a Guinier term and a power-law function [29] $G_i = c_i V_i \Delta SLD_i^2$ is the exponential prefactor (where $V_i$ is the volume of the particle and $\Delta SLD_i$ is the scattering length density (SLD) contrast existing between the $i^{th}$ structural feature and the surrounding solvent), $R_{g.i}$ is the radius of gyration describing the average size of the $i^{th}$ level structural feature and $B_i$ is a q-independent prefactor specific to the type of power-law scattering with power-law exponent, $P_i$.

The obtained values from the fitting coefficients are those that minimize the value of Chi-squared, which is defined as:

$$X^2 = \sum \left(\frac{y - y_i}{\sigma_i}\right)^2 \quad (2)$$

where $y$ is a fitted value for a given point, $y_i$ is the measured data value for the point and $\sigma_i$ is an estimate of the standard deviation for $y_i$. The curve fitting operation is carried out iteratively and for each iteration, the fitting coefficients are refined to minimize $X^2$.

### 2.9. Rheological measurements

Rheological measurements were performed on a stress-controlled rheometer (Discovery HR 20, TA Instruments, USA). The plate-plate

was used as the measurement system (upper plate 40 mm diameter with solvent trap), and a gap of 1 mm was set, to account for the size of the largest particles. The measurements were performed at 25 °C. Dispersions were loaded onto the rheometer and, kept for 60 s at 25 °C prior to the measurements. The linear viscoelastic region (LVR) was determined by performing a strain sweep from 0.01 to 1000 % at a constant angular frequency of 10 rad·s$^{-1}$. The viscoelastic behaviour was measured by small amplitude oscillatory shear at a constant shear strain of 1 % selected from the LVR and using a frequency sweep from 0.6 to 62 rad·s$^{-1}$. From these measurements, the elastic modulus G′ and the viscous modulus G″ were obtained. All measurements were performed in duplicate. A fresh sample was loaded onto the rheometer for each measurement. Data obtained from the frequency sweep were fitted by a power law model to determine the frequency dependence of G′ (Eq. (3)) and G″ (Eq. (4)):

$$G' = a\omega^c \tag{3}$$

$$G'' = b\omega^d \tag{4}$$

where $\omega$ is the angular frequency (rad/s) and a, b, c and d are model parameters.

Shear viscosity was obtained by using a steady state measurement with logarithmically increasing shear rate from 0.1 to 100 s$^{-1}$. The shear viscosity of the serum phase was measured with the same protocol using a cone geometry (40 mm diameter and 1.59° truncation, gap 52 μm). Samples were measured in duplicates. Flow curves were fitted to a power law model (Eq. 5) to determine consistency and flow behaviour index of the dispersions:

$$\sigma = K\dot{\gamma}^n \tag{5}$$

With $\sigma$ representing the shear stress (Pa), $\dot{\gamma}$ is the shear rate (s$^1$), K the consistency coefficient (Pa·s$^n$), and n the flow behaviour index.

The applicability of the Cox-Merz rule (6) was evaluated to determine the nature of the systems [30].

$$\eta(\dot{\gamma}) = |\eta^*(\omega)|_{\omega=\dot{\gamma}} \tag{6}$$

where $\eta(\dot{\gamma})$ is the shear viscosity and $\eta^*(\omega)$ is the complex viscosity measured at a small oscillatory strain.

### 2.10. Statistical analysis

Two-way ANOVA was employed to evaluate the effect of treatment, kind of seaweed and their interaction. *t*-Test for independent variables was used to detect differences between seaweed. One-way ANOVA test was used with Tukey test to compare variations in particle size as function of processing for each seaweed (confidence interval of 95 %). "R" was the open software used for all statistical analysis [31].

## 3. Results and discussion

### 3.1. Chemical composition of Laminaria digitata and Saccharina latissima

Table 1 presents the overall chemical composition of the seaweeds. The average content of protein was 7.75 % and 9.17 % (% dry weight) for LD and SL, respectively. These values agree with previous values reported for these species of seaweed, which were between 4.9–8.2 % for LD and 5.1–9.9 % for SL, depending on the season of the year [32,33], and between 1.1 % and 7.5 % for both LD and SD depending on water salinity [34].

The total fat was <2 % for both species, previous studies showed values between 1 and 3 % fat for these seaweeds [33,35–37]. The main components, ca. 60–70 %, of the seaweeds were carbohydrates (calculated by the difference between the total weight and all other non-carbohydrate components), in agreement with data previously published for these seaweeds, with values of 70.7 ± 11.6 % for LD and 63.1 ± 11.4 % for SL [32]. Ash content was 21 % and 28 % for LD and SL, respectively in the range of previously assessed values [34].

**Table 1**
Dry matter (g/100 g), protein, fat, carbohydrates, ash and phenols content of *Laminaria digitata* (LD) and *Saccharina latissima* (SL), expressed as percentage of dry matter (%), except for total phenols (mg/100 g). Mean ± standard deviation ($n = 3$).

| | LD | SL |
|---|---|---|
| Dry matter | 91.12 ± 0.07 | 89.94 ± 0.03 |
| Protein[a] | 7.75 ± 0.26 | 9.17 ± 0.02 |
| Fat | 1.95 ± 0.11 | 1.39 ± 0.11 |
| Carbohydrates | 69.07 ± 0.13 | 60.68 ± 0.07 |
| Ash | 21.23 ± 0.01 | 28.76 ± 0.09 |
| Phenols | 100.97 ± 6.49 | 127.2 ± 3.21 |

[a] Protein values are calculated using a conversion factor of 5.6.

The content of total phenols was 100 mg/100 g and 127 mg/100 g for LD and SL respectively. For LD, values were similar to those reported by Schiener et al. [32], of approximately 150 mg/100 g. However, for SL the values were lower than those previously measured (ca. 450 mg/100 g). Variability in total phenols could be due to biological differences between the seaweeds used in the studies.

### 3.2. Monosaccharide composition of Laminaria digitata and Saccharina latissima

The monosaccharide analysis (Fig. 2) indicated that the main neutral sugars in the LD and SL powders were glucose (ca. 52–61 %) and fucose (ca. 7.6–11 %) representing mainly laminarins ((1–3-)-$\beta$-D-glucan) and fucoidans. The main uronic acids were mannuronic acid (ManA) and guluronic acid (GulA), accounting for 18.4 % of the LD and 28.4 % of the SL, attributed to alginate. Galactose (Gal) was also ascribed to fucoidan with branches of xylose (Xyl) and mannose (Man) [38]. Glucuronic acid (GluA) was below 1 mg/g. The monosaccharide profile of the seaweed powders agrees with previous studies [18,39]. All dispersions showed similar monosaccharide profile to the seaweed powders, indicating no losses during processing (Supplementary Material Fig. S1).

### 3.3. Effect of processing on the solubilisation of polysaccharides

In order to understand the impact of processing on polysaccharides solubilisation, the serum of each dispersion was separated by centrifugation and, the monosaccharides composition was analysed (Fig. 2). The main components in the serum phase are polysaccharides, as protein content in these seaweed species is relatively low (<10 % wt.) as shown in Table 1. Furthermore, it has been reported that extraction of proteins from these brown seaweed species is challenging because they are strongly interacting with cell wall polysaccharides [5]. Some minerals and vitamins could be also solubilised in the water; however, in comparison to the polysaccharides their contribution to the structuring ability and rheological properties would be negligible.

The serum of untreated samples showed the presence of Fuc, Gal, Glu, Man, ManA and GulA, attributed to solubilisation of fucoidan, laminarin and alginate in the water. Whilst the Glu content in the powders and dispersions would be related to laminarin and cellulose, in the sera it would be only from laminarin, as cellulose would remain in the pellet after centrifugation. In sera from SL, Glu was lower compared to LD, suggesting a lower solubilisation of laminarin. The thermal treatment seemed to induce further solubilisation of laminarin in SL.

The addition of a high pressure homogenisation step led to sera with similar monosaccharide profile than prior to homogenisation, independently of homogenisation temperature. Thus, considering the relative composition of monosaccharides, the sera of LD samples which were thermally treated contained 28 % fucoidan, 2.3 % alginate and 69 %

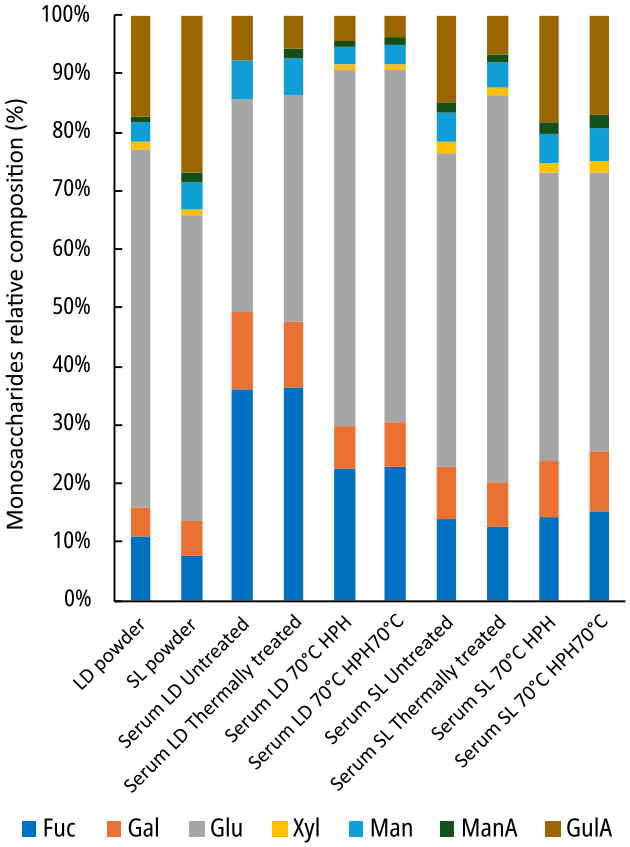


**Fig. 2.** Relative composition of monosaccharides (%) in the seaweed powders and serum phases obtained after centrifugation of processed dispersions. LD = *Laminaria digitata*, SL = *Saccharina latissima*; Fuc = fucose; Gal = galactose, Glu = glucose; Xyl = xylose; Man = mannose; GulA = guluronic acid; ManA = mannuronic acid. 70 °C HPH = thermal treatment at 70 °C followed by high pressure homogenisation at room temperature; 70 °C HPH70 °C = thermal treatment at 70 °C followed by high pressure homogenisation at 70 °C.

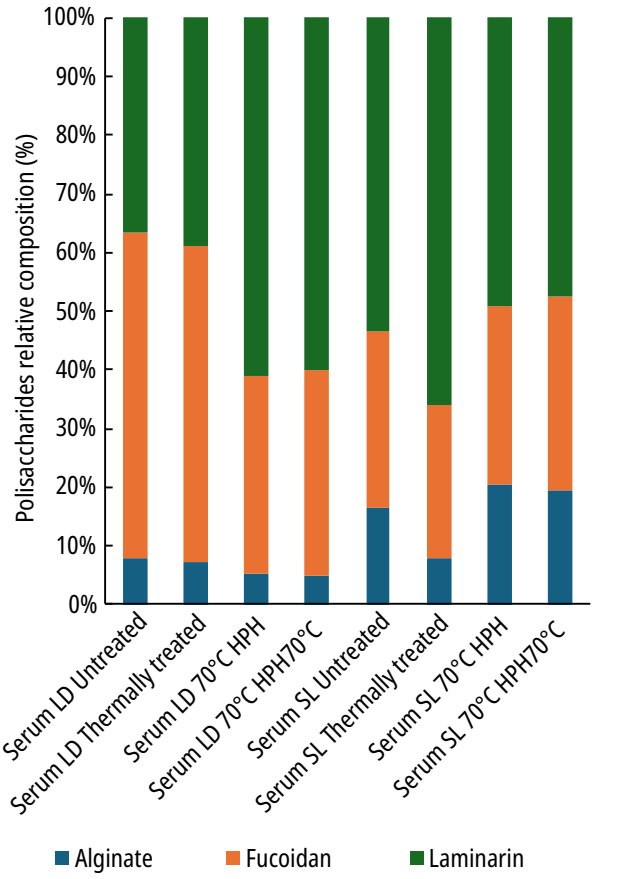


**Fig. 3.** Relative composition of polysaccharides (%) in serum phases. LD = *Laminaria digitata*, SL = *Saccharina latissima*. 70 °C HPH = thermal treatment at 70 °C followed by high pressure homogenisation at room temperature; 70 °C HPH70 °C = thermal treatment at 70 °C followed by high pressure homogenisation at 70 °C. Polysaccharides are calculated as: alginate = ManA + GulA; laminarin = Glu; fucoidan = Fuc + Gal + Xyl + Man + GlcA.

laminarin (Fig. 3). Addition of a HPH step led to sera with 38–41 % fucoidan, 2 % alginate and 56–59 % laminarin, indicating that the HPH led to sera enriched in fucoidan. In the case of SL, the composition of thermally treated sera was 29 % fucoidan, 7 % alginate and 63 % laminarin. The addition of the HPH step exhibited sera with composition percentages of 34–37 % fucoidan, 18–19 % alginate and 44–47 % laminarin, showing that the sera were enriched in fucoidan and alginate.

### 3.4. Effect of processing on the microstructure of seaweed dispersions

Fig. 4A represents the effect of processing on the particle size distribution of the seaweed dispersions, showing a statistically significant reduction in particle size as result of high pressure homogenisation (Table 2). HPH led to a reduction in surface base diameter ($D_{[3,2]}$) of approximately twelve times for both species, from approximately 300–400 μm to 20–30 μm. Similar particle size was obtained independently of the application of a thermal treatment (prior to HPH or during HPH). Furthermore, both species showed similar behaviour. This reduction in particle size is greater than that reported by Malafronte et al. [18] for LD, with a reduction of only 2.5 times using equally intense shear treatment. The differences were attributed to the initial sieving process applied in the current study, which reduced the initial particle size and, thus, the energy input required for particle breakage by the HPH process [40]. The morphology of the particles was visualised by confocal laser scanning microscopy (Fig. 4B), a change in particle shape was clearly observed, being large irregular clusters of cells before HPH and, single cells and broken cell fragments after HPH.

### 3.5. Effect of processing on the nanostructure of seaweed dispersions

To understand the structural changes taking place at the nanoscale, the seaweed powders and the dispersions obtained after the thermal and mechanical treatments were characterised by small angle X-ray scattering (SAXS) and, the obtained scattering patterns are shown in Fig. 5. From the scattering patterns of the seaweed dispersions (Fig. 5A and B), it is evident that the applied treatments had a much stronger effect on LD than on SL. While in the case of SL procesing only had a minor effect on the scattering intensity of the samples (Fig. 5B), major changes in the intensity and shape of the scattering patterns were observed in the LD processed samples. As evidenced by the scattering patterns from the dispersions after being freeze-dried, the HPH treatment led to a reduction in the intensity from LD, which may be indicative of a decrease in the packing density of the cell wall structures found at the nanoscale level (Fig. 5A). This effect was stronger when a thermal treatment was applied prior to HPH. In the case of SL, only the combination of thermal and HPH treatments seemed to have a significant effect on the nanoscale structure of the cell walls (Fig. 5B).

Interestingly, the scattering patterns of the serum phase from the SL samples after the application of HPH show a very weak shoulder, indicating that some compounds from the seaweed cell walls were solubilised in the aqueous phase (Fig. 5D). These shoulder features were much more evident in the case of the LD serum samples, suggesting a greater solubilisation of cell wall components in that case (Fig. 5C). Furthermore, while the intensity of the curves from all the serum samples from SL was very similar, differences were evident among the serum samples

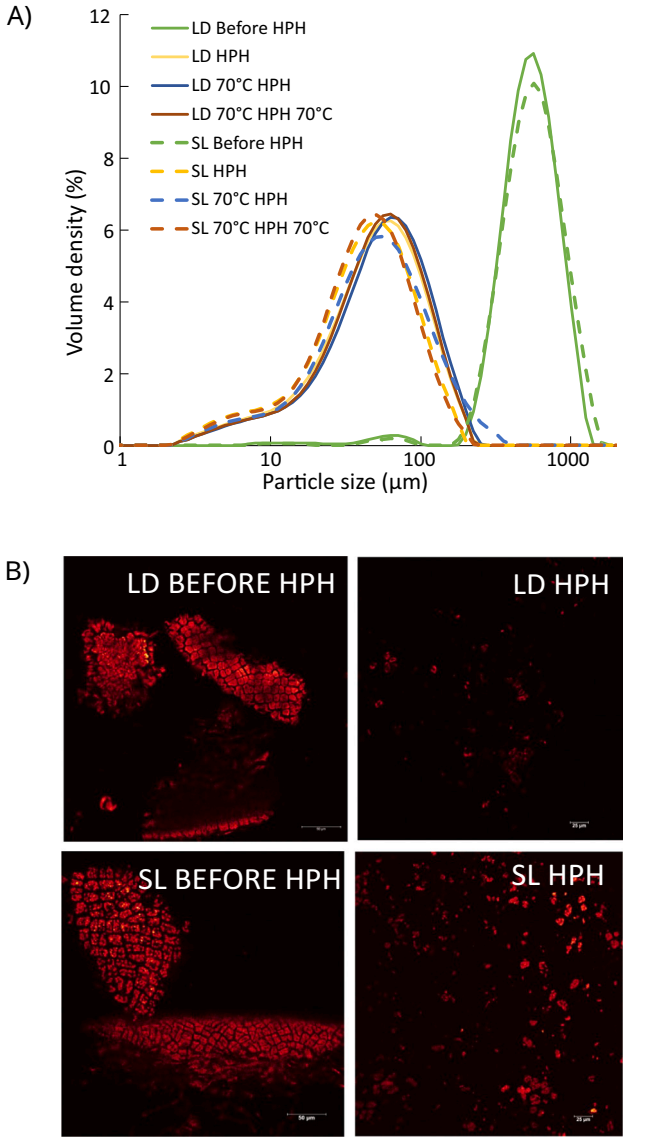


**Fig. 4.** A) Volume density vs particle size curves of brown seaweed dispersions. *Laminaria digitata* (LD) and *Saccharina latissima* (SL), before and after high pressure homogenisation (HPH); after thermal treatment at 70 °C followed by homogenisation at room temperature (70 °C HPH) and, after thermal treatment at 70 °C followed by homogenisation at 70 °C (70 °C HPH 70 °C). B) Micrographs illustrating particle morphology before and after high pressure homogenisation, obtained by confocal scanning laser microscopy.

obtained from LD after different treatments. This suggests that the cell walls from LD are more labile and cell wall components can be solubilised more easily than in the case of SL. Previous work reported the appearance of similar, although more intense, shoulder-like features in sodium alginate solutions extracted from SL through the application of a high hydrostatic pressure pretreatment [41]. In line with that work, the data from the present study were fitted using an empirical Beaucage model (also known as unified model) and the obtained fitting parameters are summarised in Table 3. As observed, very small differences were noted in the fitting parameters for the serum samples from SL. Within the high q region, all the samples showed power-law exponents close to 1, which is indicative of the existence of rod-like structures at the corresponding size range, and the associated radii of gyration were 4–6 nm.

Thus, the molecular chains of the solubilised polysaccharides seemed to be in an extended rod-like conformation in all the serum samples. At the next structural level, the samples presented power-law exponents

**Table 2**
Surface base diameter ($D_{[3,2]}$) for each process (95 % confidence). LD (*Laminaria digitata*); SL (*Saccharina latissima*); HPH (High Pressure Homogenisation). NS (not significant); (p>0.05); *p≤0.05; **p≤0.01; ***p≤0.001. Significant differences in a column are indicated with different superscript letters.

| | | LD $D_{[3,2]}$ ($\mu m$) | SL $D_{[3,2]}$ ($\mu m$) |
|---|---|---|---|
| Treatment | Before HPH | $344.22 \pm 65.79^{a}$ | $396.68 \pm 47.30^{a}$ |
| | HPH | $27.16 \pm 0.47^{b}$ | $23.33 \pm 0.84^{b}$ |
| | 70 °C HPH | $29.17 \pm 1.64^{b}$ | $26.65 \pm 0.15^{b}$ |
| | 70 °C HPH 70 °C | $28.41 \pm 0.97^{b}$ | $27.42 \pm 1.47^{b}$ |
| | | LD vs SL | |
| ANOVA two-way | Seaweed | NS | |
| | Treatment | *** | |
| | Interaction | NS | |
| T-test | Before HPH | NS | |
| | HPH | ** | |
| | 70 °C HPH | NS | |
| | 70 °C HPH 70 °C | NS | |
| ANOVA one-way | *p*-Value | *** | *** |

indicative of fractal structures. In the case of the SL samples, the power-law exponents increased from 3 to 4 after the thermal treatment, but in general the associated radii of gyration were very similar (14–16 nm). This structural level may be related to the intermolecular association of the individual polysaccharide chains, which were arranged forming an intertwined network of clusters. In the case of the LD samples, the power-law exponents also increased after the thermal treatment, and the radii of gyration increased from 17 nm to 30–31 nm for the samples subjected to either HPH or thermal treatment, while it decreased down to 15 nm for the sample combining the thermal and HPH treatments. In the low q region, the SL samples presented power-law exponents close to 3, indicating the existence of highly clustered networks, and the associated radii of gyration were 77–83 nm. This structural level may be associated to the arrangement of polysaccharide clusters into an intertwined network, similar to that found in gel-like structures. This could be explained by the greater proportion of alginate in the serum phases from this seaweed (Fig. 2). In the case of the LD samples, the radii of gyration were 71–77 nm and the power-law exponents decreased from 3 to 1 for the HPH or thermally treated samples, while it increased back to 3 for the sample combining both treatments. This indicates that a structural conformation was obviously taking place in the LD HPH and thermally treated samples, probably because a greater amount of polysaccharides was being released towards the serum phase.

### 3.6. *Effect of processing on the viscoelastic behaviour of the seaweed dispersions*

Rheological behaviour of the seaweed dispersions was evaluated via strain and frequency sweeps. Only high pressure homogenised dispersions could be measured, as non-homogenised samples quickly sedimented. This observation already indicated the potential of HPH to functionalise seaweed dispersions. Fig. 6A and B represent the elastic and viscous moduli as function of the applied strain. This experiment revealed the linear viscoelastic region of the dispersions, represented by a plateau up to approximately 10 % oscillation strain for both types of seaweed.

Results showed that all dispersions presented similar viscoelastic properties independently of the application of a thermal treatment at 70 °C, prior or during the high-pressure homogenisation step. The value of $G'$ provides information on the stiffness of the structure, for LD the $G'$ at 1 % strain was 145 ± 0.8 Pa, 145 ± 20 Pa and 191 ± 6.8 Pa for LD HPH, LD 70 °C HPH and LD 70 °C HPH 70 °C respectively, indicating that all networks had similar stiffness. The viscoelastic behaviour is determined by the phase angle $\delta$ (given by $tan\delta = G''/G'$) and had values of $< 45°$ for all LD dispersions indicating a predominant elastic behaviour. For SL the $G'$ at 1 % strain was 173 ± 16 Pa, 206 ± 5 Pa and 159 ±

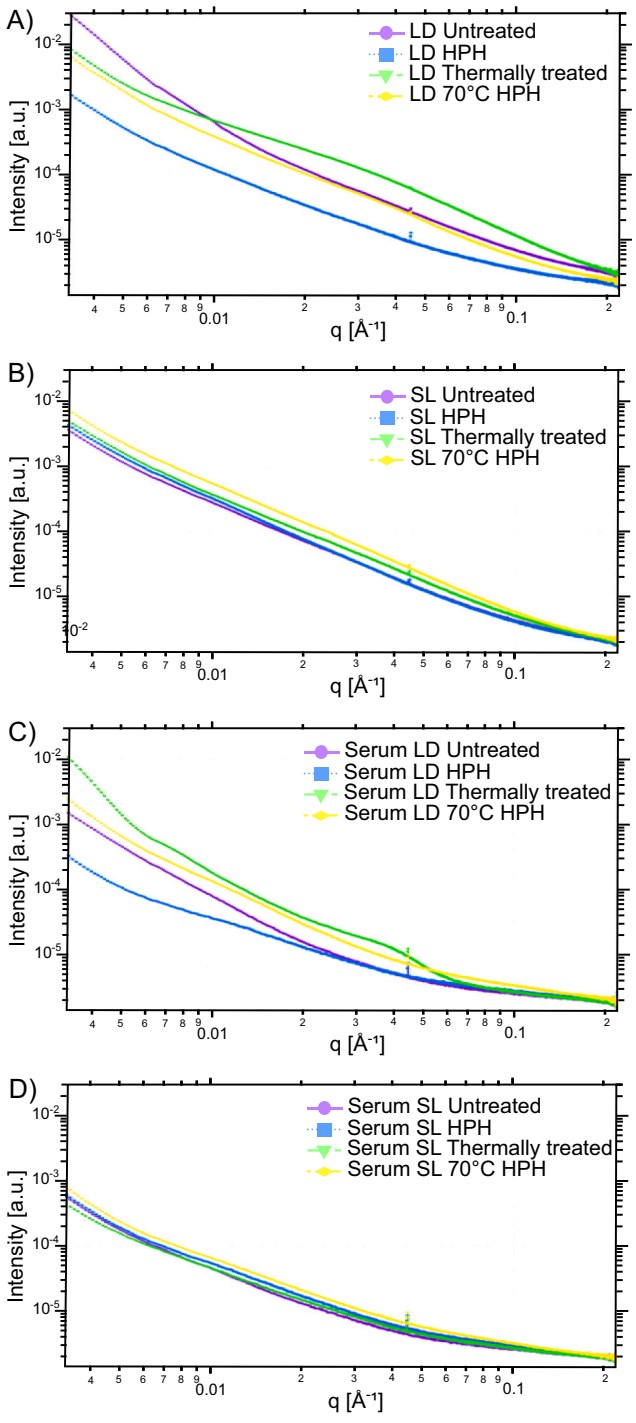


**Fig. 5.** SAXS patterns of whole dispersions (A and B) and of the serum phase obtained after centrifugation (C and D) for *Laminaria digitata* (LD) and *Saccharina latissima* (SL) samples.

12 Pa for SL HPH, SL 70 °C HPH and SL 70 °C HPH 70 °C respectively, indicating that all networks had similar stiffness between them and similar to LD. The phase angle had values of <45° for all SL dispersions. The gel- like behaviour of LD and SL dispersions after HPH was thus indicated by the values of G′ and phase angle.

The network structure was further characterised by frequency sweep measurements (Fig. 6C and D), to study the dependence of G′ and G″ on the angular frequency. The frequency sweeps were fitted by a power law model. Table 4 summarises the parameters obtained from the power law fitting. The dispersions showed similar values of c and d, with values

**Table 3**
Parameters obtained from the fits of the SAXS data ($R_{gi}$: radius of gyration for the structural level i; $P_i$: power-law exponent for the structural level i. LD = *Laminaria digitata*, SL = *Saccharina latissima*, HPH = High pressure homogenisation).

| Sample | Treatment | $P_1$ | $R_{g1}$(nm) | $P_2$ | $R_{g2}$(nm) | $P_3$ | $R_{g3}$(nm) |
|---|---|---|---|---|---|---|---|
| Serum LD | Untreated | 2.8 | 71.5 | 2.8 | 17.2 | 1.0 | 4.0 |
| | HPH | 1.3 | 71.0 | 2.4 | 29.9 | 1.0 | 5.6 |
| | Thermally treated | 1.0 | 75.9 | 3.8 | 31.1 | 1.0 | 5.2 |
| | 70 °C HPH | 2.9 | 76.7 | 3.6 | 14.5 | 1.3 | 4.7 |
| Serum SL | Untreated | 2.7 | 77.7 | 2.6 | 16.3 | 1.0 | 4.5 |
| | HPH | 2.8 | 77.0 | 3.2 | 14.0 | 1.0 | 5.1 |
| | Thermally treated | 2.7 | 80.0 | 4.0 | 16.2 | 1.1 | 5.8 |
| | 70 °C HPH | 3.2 | 82.6 | 4.0 | 14.9 | 1.0 | 5.3 |

ranging between 0.12 and 0.16 for c, and between 0.20 and 0.25 for d, indicating similar frequency dependence for all samples. Furthermore, G′ was larger than G″ over the whole range of frequencies, this rheological behaviour is typical of weak gels [42]. Parameters a and b were also of the same magnitude for all dispersions, indicating that the formed networks were of similar strength. The presence of alginate and divalent cations (in particular $Ca^{2+}$) in the seaweed could contribute to the strength of the network, as alginate is able to gel in the presence of cations. The content of $Ca^{2+}$ in LD was measured to be ca. 19,700 mg/kg and in SL was ca. 18,000 mg/kg.

### 3.7. Effect of processing on the flow behaviour of the seaweed dispersions

Fig. 7 shows that aqueous dispersions after high-pressure homogenisation had shear thinning behaviour (i.e. viscosity decreased with shear rate). The shear stress vs. shear rate curves were fitted using a power-law model, as no evidence for the existence of yield stress was observed. All the dispersions showed n <1, with values between 0.13 and 0.34 (Table 5). The lowest values corresponded to the samples without thermal treatment, with $n = 0.21 \pm 0.01$ for LD and $n = 0.13 \pm 0.00$ for SL. Furthermore, the goodness of the fitting was poor for SL ($R^2 = 0.82$), indicating that phase separation or sedimentation could be interfering with the viscosity measurements. All samples showed similar consistency with values between 15.38 and 22.6 $Pa{\cdot}s^{-n}$. Since all dispersions had similar particle size distribution (Fig. 4A) and composition (Supplementary Material Fig. S1), the results suggests that the contribution of hydrodynamic forces was similar in all the samples. Thus the flow behaviour of the dispersions was driven by the homogenisation process, whilst the type of seaweed species and the thermal treatment were less determinant of their flow behaviour.

### 3.8. Effect of processing on the serum viscosity

One of the parameters influencing the rheological properties of a dispersion is the viscosity of the continuous phase. Fig. 8 depicts the shear viscosity of the sera separated by centrifugation. The samples which were not thermally treated (serum LD HPH and SL HPH) had a sera with a Newtonian behaviour and viscosity of approximately 0.002 Pa·s at 10 $s^{-1}$, close to water. The thermal treatment prior to HPH led to an increase in viscosity for both seaweed however, SL (0.02 Pa·s at 10 $s^{-1}$) showed a larger increase in viscosity compared to LD (0.009 Pa·s at 10 $s^{-1}$), and also a change in behaviour from Newtonian to shear thinning. Increasing the temperature at which the high pressure homogenisation was performed did not impact the viscosity of the serum. The total solids content of the sera was ca. 2–2.5 % for LD and 3 % for SL. Furthermore, the sera of SL were richer in alginate, compared to LD (Fig. 2), this could explain the shear thinning behaviour and higher viscosity of the sera from SL. These results indicate that the combination of heating and high shear increase solubilisation of cell components, which contribute to the rheology of the serum phase,

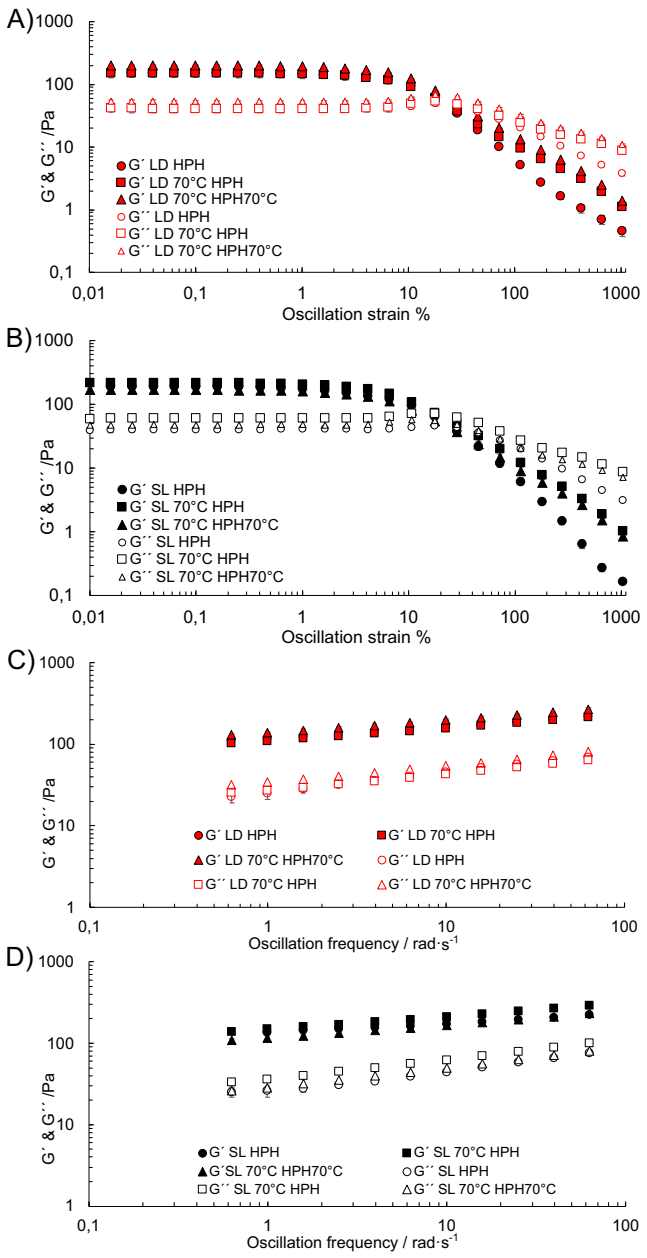


**Fig. 6.** Strain sweep curves at a constant angular frequency of 10 rad·s$^{-1}$ for aqueous dispersions (5 % *w/v*) of *Laminaria digitata* (A) and *Saccharina latissima* (B). Frequency sweep curves at a constant shear strain of 1 % for *Laminaria digitata* (C) and *Saccharina latissima* (D). Data points are the average of two measurements. Error bars are also represented although not visible at the scale selected.

furthermore this effect seemed to be larger in SL compared to LD. Nevertheless, the differences observed in sera viscosity were not reflected in changes in the overall viscosity of the dispersions (Fig. 7), indicating that at the concentrations studied, the flow behaviour was determined by the phase volume occupied by the particles.

### 3.9. Applicability of the Cox Merz rule

The dispersions were further studied by application of the Cox–Merz rule [30]. The Cox-Merz rule in rheology suggests that dynamic viscosity is equivalent to steady-state viscosity for certain materials under specific conditions, reflecting a stable microstructure. In polymer systems, this equivalence implies well-aligned chains and consistent interactions. The shear viscosity was lower than complex viscosity for all dispersions (Fig. 9), indicating that they did not follow the Cox–Merz rule, allowing the conclusion that the systems did not behave as macromolecules in solution but rather as suspensions of soft "seaweed" particles. Whilst weak gels could be the result of covalent and non-covalent molecular

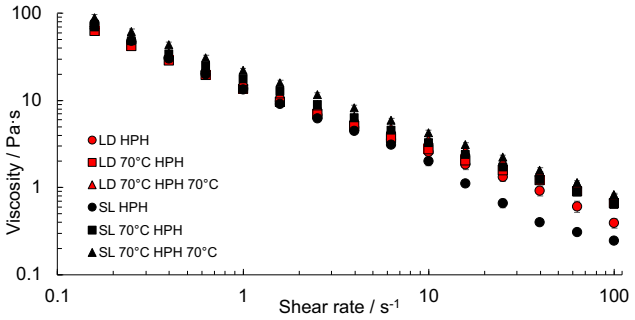


**Fig. 7.** Shear viscosity curves of aqueous dispersions (5 % w/v) of LD (*Laminaria digitata*) and SL (*Saccharina latissima*). HPH (high pressure homogenisation), 70 °C HPH (thermal treatment at 70 °C followed by HPH at room temperature) and, 70 °C HPH 70 °C (thermal treatment at 70 °C followed by HPH at 70 °C).

**Table 5**
Parameters obtained from the power law fitting of the shear stress vs shear rate data. n represents the flow index and k consistency. LD (*Laminaria digitata*), SL (*Saccharina latissima*). HPH (high pressure homogenisation), 70 °C HPH (thermal treatment at 70 °C followed by HPH at room temperature) and, 70 °C HPH 70 °C (thermal treatment at 70 °C followed by HPH at 70 °C).

| Seaweed | Treatment | Consistency coefficient (Pa·s$^{-n}$) | Flow behaviour (−) | $R^2$ |
|---|---|---|---|---|
| LD | HPH | 15.48 ± 1.66 | 0.21 ± 0.00 | 0.97 |
| | 70 °C HPH | 15.38 ± 2.77 | 0.31 ± 0.03 | 0.98 |
| | 70 °C HPH 70 °C | 17.25 ± 0.72 | 0.34 ± 0.01 | 0.99 |
| SL | HPH | 16.51 ± 2.32 | 0.13 ± 0.00 | 0.82 |
| | 70 °C HPH | 17.53 ± 0.00 | 0.28 ± 0.01 | 0.99 |
| | 70 °C HPH 70 °C | 22.6 ± 1.61 | 0.28 ± 0.00 | 0.99 |

**Table 4**
Parameters a, b, c and d of the power law models ($G' = a{\cdot}\omega^c$ and $G'' = b{\cdot}\omega^d$) fitted to the storage modulus (G′) and loss modulus (G″) as a function of the angular frequency ($\omega$) ($R^2 = 0.99$). LD (*Laminaria digitata*), SL (*Saccharina latissima*). HPH (high pressure homogenisation), 70 °C HPH (thermal treatment at 70 °C followed by HPH at room temperature) and, 70 °C HPH 70 °C (thermal treatment at 70 °C followed by HPH at 70 °C).

| | Treatment | a | b | c | d |
|---|---|---|---|---|---|
| LD | HPH | 115.92 ± 16.0 | 25.56 ± 4.30 | 0.15 ± 0.00 | 0.25 ± 0.01 |
| | 70 °C HPH | 109.62 ± 8.00 | 27.30 ± 2.29 | 0.16 ± 0.00 | 0.20 ± 0.01 |
| | 70 °C HPH 70 °C | 138.87 ± 3.73 | 34.21 ± 0.58 | 0.16 ± 0.00 | 0.20 ± 0.00 |
| SL | HPH | 140.55 ± 13.32 | 25.56 ± 2.36 | 0.12 ± 0.00 | 0.25 ± 0.01 |
| | 70 °C HPH | 146.66 ± 0.900 | 36.08 ± 0.09 | 0.16 ± 0.00 | 0.24 ± 0.00 |
| | 70 °C HPH 70 °C | 114.70 ± 3.500 | 28.36 ± 0.41 | 0.16 ± 0.00 | 0.25 ± 0.00 |

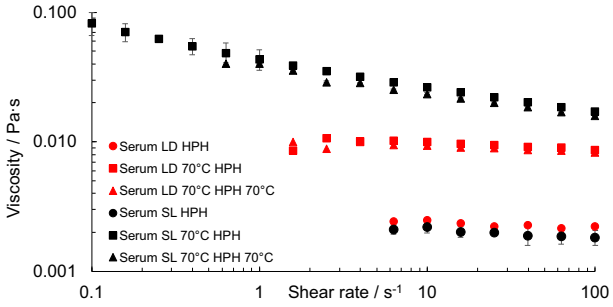


**Fig. 8.** Shear viscosity curves of the serum phase obtained from centrifugation of the seaweed dispersions.LD (*Laminaria digitata*), SL (*Saccharina latissima*). HPH (high pressure homogenisation), 70 °C HPH (thermal treatment at 70 °C followed by HPH at room temperature) and, 70 °C HPH 70 °C (thermal treatment at 70 °C followed by HPH at 70 °C).

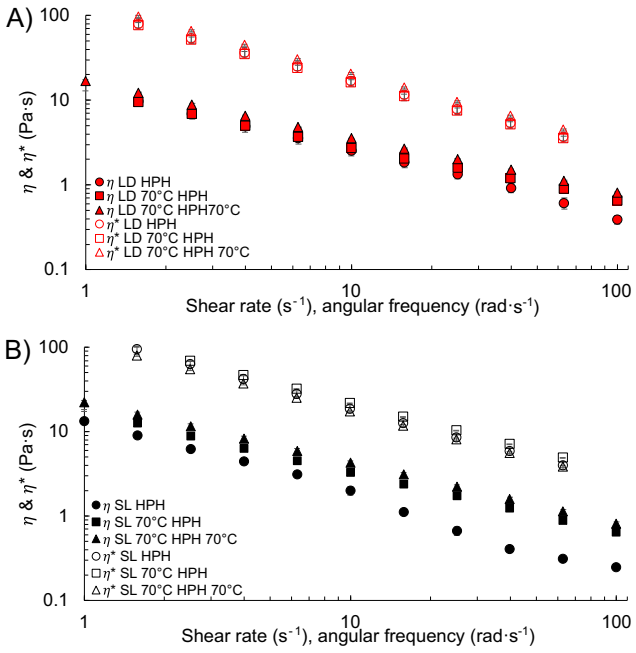


**Fig. 9.** Cox-Merz rule comparison of shear viscosity $\eta$ (full symbols) and complex viscosity $\eta^*$ (empty symbols) as a function of shear rate and frequency, respectively, for LD (*Laminaria digitata*) (A) and SL (*Saccharina latissima*) dispersions (B). HPH (high pressure homogenisation), 70 °C HPH (thermal treatment at 70 °C followed by HPH at room temperature) and, 70 °C HPH 70 °C (thermal treatment at 70 °C followed by HPH at 70 °C).

crosslinks [43], it is clear than in these dispersions the gel like nature arises from the interactions between seaweed particles.

## 4. Conclusions

We concluded that aqueous dispersions of whole *Laminaria digitata* and *Saccharina latissima* hold the potential to be used as natural texturisers in semiliquid food products, by applying high shear treatments such as high pressure homogenisation. Processed *Laminaria digitata* cell walls were less dense than prior to processing, which was linked to the release of greater amounts of structural polysaccharides, such as fucoidan and alginate. The nanostructure of *Saccharina latissima* cell walls was less affected by processing conditions, despite larger amounts of alginate being released, suggesting that these two species might present different structural organisation in their cell walls. The dispersions exhibited complex flow behaviour, with characteristics such as shear-thinning, attributed mainly to interactions between soft seaweed particles. Solubilisation of cell wall polysaccharides increased the viscosity of the serum phase, this effect seemed to be larger in *Saccharina latissima* compared to *Laminaria digitata*, due to a higher content of alginate in the serum of the *Saccharina latissima*. However, such differences in sera viscosity were not reflected in the rheology of the dispersions, which were mainly dominated by the dispersed phase. Although other organoleptic factors such as colour and flavour profile must be investigated, from a rheological point of view our results support the utilisation of these marine biomass as natural structurants in food products.

Supplementary data to this article can be found online at https://doi.org/10.1016/j.algal.2024.103548.

## CRediT authorship contribution statement

**Antonio Souto-Prieto:** Writing – original draft, Visualization, Investigation, Formal analysis, Data curation. **Marta Martinez-Sanz:** Writing – review & editing, Writing – original draft, Visualization, Investigation, Formal analysis, Data curation. **Tania Ferreiro:** Writing – review & editing, Investigation, Formal analysis. **Patricia Parada-Pena:** Writing – original draft, Investigation. **Laura Abuin-Arias:** Writing – original draft, Investigation. **Angel Cobos:** Writing – review & editing, Writing – original draft, Supervision, Methodology, Formal analysis. **Patricia Lopez-Sanchez:** Writing – review & editing, Writing – original draft, Supervision, Project administration, Methodology, Funding acquisition, Formal analysis, Conceptualization.

## Declaration of competing interest

The authors have declared that no competing interests exist.

## Data availability

Data will be made available on request.

## Acknowledgments

The authors are grateful to Verónica Piñeiro Gómez (RIAIDT, Universidade de Santiago de Compostela, Campus Lugo) for her technical expertise on monosaccharide analysis. The research leading to these results was supported by Project TED2021-130352B-I00 (Ministerio de Ciencia e Innovación, Spain); and Ramon y Cajal fellowship RYC2020-030485-I (Ministerio de Ciencia e Innovación, Spain). Antonio Souto-Prieto is the holder of a research contract 17DF-D5BD-4071-A710 (Campus Terra, Xunta de Galicia, Spain).

## References

[1] C.J. Diaz, K.J. Douglas, K. Kang, A.L. Kolarik, R. Malinovski, Y.R. Torres-Tiji, J. V. Molino, A. Badary, S.P. Mayfield, Developing algae as a sustainable food source, Front. Nutr. 9 (2023) 1029841, https://doi.org/10.3389/fnut.2022.1029841.

[2] P. Cherry, C. O'Hara, P.J. Magee, E.M. McSorley, P.J. Allsopp, Risks and benefits of consuming edible seaweeds, Nutr. Rev. 77 (2019) 307–329, https://doi.org/10.1093/nutrit/nuy066.

[3] S. Roohinejad, M. Koubaa, F.J. Barba, S. Saljoughian, M. Amid, R. Greiner, Application of seaweeds to develop new food products with enhanced shelf-life, quality and health-related beneficial properties, Food Res. Int. 99 (2017) 1066–1083, https://doi.org/10.1016/j.foodres.2016.08.016.

[4] M. Gordalina, H.M. Pinheiro, M. Mateus, M.M.R. da Fonseca, M.T. Cesário, Macroalgae as protein sources—a review on protein bioactivity, extraction, purification and characterization, Appl. Sci. 11 (2021), https://doi.org/10.3390/app11177969. URL: https://search.proquest.com/docview/2570582679.

[5] H. Harrysson, M. Hayes, F. Eimer, N.G. Carlsson, G.B. Toth, I. Undeland, Production of protein extracts from swedish red, green, and brown seaweeds, porphyra umbilicalis kutzing, ulva lactuca linnaeus, and saccharina latissima (linnaeus) j. v. lamouroux using three different methods, J. Appl. Phycol. 30 (2018) 3565–3580, https://doi.org/10.1007/s10811-018-1481-7.

[6] E. Deniaud-Bouet, N. Kervarec, G. Michel, T. Tonon, B. Kloareg, C. Herve, Chemical and enzymatic fractionation of cell walls from fucales: insights into the structure of the extracellular matrix of brown algae, Ann. Bot. 114 (2014) 1203–1216, https://doi.org/10.1093/aob/mcu096.

[7] Z.A. Popper, G. Michel, C. Herve, D.S. Domozych, W.G.T. Willats, M.G. Tuohy, B. Kloareg, D.B. Stengel, Evolution and diversity of plant cell walls: from algae to flowering plants, Annu. Rev. Plant Biol. 62 62 (2011), https://doi.org/10.1146/annurev-arplant-042110-103809 (567–+).
[8] G.L. Naylor, B. Russell-Wells, On the presence of cellulose and it's distribution in the cell-walls of brown and red algae, Ann. Bot. 48 (1934) 635–641, https://doi.org/10.1093/oxfordjournals.aob.a090468.
[9] G.T. Grant, E.R. Morris, D.A. Rees, P. Smith, D. Thom, Biological interactions between polysaccharides and divalent cations - egg-box model, FEBS Lett. 32 (1973) 195–198, https://doi.org/10.1016/0014-5793(73)80770-7.
[10] C. Hu, W. Lu, A. Mata, K. Nishinari, Y. Fang, Ions-induced gelation of alginate: mechanisms and applications, Int. J. Biol. Macromol. 177 (2021) 578–588, https://doi.org/10.1016/j.ijbiomac.2021.02.086.
[11] A. Rodriguez-Bernaldo, J. Lopez-Hernandez, An overview on effects of processing on the nutritional content and bioactive compounds in seaweeds, Foods 10 (2021) 2168, https://doi.org/10.3390/foods10092168.
[12] V. Figueroa, M. Farfán, J.M. Aguilera, Seaweeds as novel foods and source of culinary flavors, Food Rev. Int. 39 (2023) 1–26. URL: https://www.tandfonline.com/doi/abs/10.1080/87559129.2021.1892749 https://doi.org/10.1080/87559129.2021.1892749.
[13] N. Francezon, A. Tremblay, J.L. Mouget, P. Pasetto, L. Beaulieu, Algae as a source of natural flavors in innovative foods, J. Agric. Food Chem. 69 (2021) 11753–11772, https://doi.org/10.1021/acs.jafc.1c04409.
[14] C. Mateluna, V. Figueroa, J. Ortiz, J.M. Aguilera, Effect of processing on texture and microstructure of the seaweed durvillaea antarctica, J. Appl. Phycol. 32 (2020) 4211–4219, https://doi.org/10.1007/s10811-020-02259-1.
[15] M. Onodera, Y. Yoshie-Stark, T. Suzuki, Changes in texture and dietary fiber of the brown alga undaria pinnatifida by various processing methods, Food Sci. Technol. Res. 14 (2008) 89–94, https://doi.org/10.3136/fstr.14.89.
[16] P. Lopez-Sanchez, J. Nijsse, H.C.G. Blonk, L. Bialek, S. Schumm, M. Langton, Effect of mechanical and thermal treatments on the microstructure and rheological properties of carrot, broccoli and tomato dispersions, J. Sci. Food Agric. 91 (2011) 207–217, https://doi.org/10.1002/jsfa.4168.
[17] T.M.M. Bernaerts, A. Panozzo, V. Doumen, I. Foubert, L. Gheysen, K. Goiris, P. Moldenaers, M.E. Hendrickx, A.M.V. Loey, Microalgal biomass as a (multi) functional ingredient in food products: rheological properties of microalgal suspensions as affected by mechanical and thermal processing, Algal Research-Biomass Biofuels and Bioproducts 25 (2017) 452–463, https://doi.org/10.1016/j.algal.2017.05.014.
[18] L. Malafronte, S. Yilmaz-Turan, A. Krona, M. Martinez-Sanz, F. Vilaplana, P. Lopez-Sanchez, Macroalgae suspensions prepared by physical treatments: effect of polysaccharide composition and microstructure on the rheological properties, Food Hydrocoll. 120 (2021) 106989, https://doi.org/10.1016/j.foodhyd.2021.106989.
[19] J. Kjeldahl, Neue methode zur bestimmung des stickstoffs in organischen körpern, Z. Anal. Chem. 22 (1883) 366–382. URL: https://doi.org/10.1007/BF01338151 (iD: Kjeldahl1883).
[20] J.V. Vilg, I. Undeland, ph-driven solubilization and isoelectric precipitation of proteins from the brown seaweed saccharina latissima-effects of osmotic shock, water volume and temperature, J. Appl. Phycol. 29 (2017) 585–593, https://doi.org/10.1007/s10811-016-0957-6.
[21] A. Purkiewicz, S. Czaplicki, R. Pietrzak-Fiecko, The occurrence of squalene in human milk and infant formula, Int. J. Environ. Res. Public Health 19 (2022) 12928, https://doi.org/10.3390/ijerph191912928.
[22] K. Liu, Effects of sample size, dry ashing temperature and duration on determination of ash content in algae and other biomass, Algal Research-Biomass Biofuels and Bioproducts 40 (2019) 101486, https://doi.org/10.1016/j.algal.2019.101486.
[23] C. Gonçalves, Estudio de compuestos bioactivos presentes en macroalgas de las costas gallegas. Estudio de compuestos bioactivos presentes en macroalgas de las costas gallegas, URL: http://hdl.handle.net/10347/18258, 2019.
[24] D. Marinova, F. Ribarova, M. Atanassova, Total phenolics and total flavonoids in bulgarian fruits and vegetables, Journal of the University of Chemical Technology and Metallurgy 40 (2005) 255–260. URL: https://cir.nii.ac.jp/crid/1570291225943829504.
[25] A. Leyton, R. Pezoa-Conte, A. Barriga, A.H. Buschmann, P. Mäki-Arvela, J. P. Mikkola, M.E. Lienqueo, Identification and efficient extraction method of phlorotannins from the brown seaweed macrocystis pyrifera using an orthogonal experimental design, Algal Res. 16 (2016) 201–208. URL: https://doi.org/10.1016/j.algal.2016.03.019.
[26] CELLS, Alba synchroton, URL, https://www.albasynchrotron.es/es, 2023.
[27] J. Kieffer, J.P. Wright, Pyfai: a python library for high performance azimuthal integration on gpu, Powder Diffract. 28 (2013) S339–S350, https://doi.org/10.1017/S0885715613000924.
[28] J. Ilavsky, P.R. Jemian, Irena: tool suite for modeling and analysis of small-angle scattering, J. Appl. Crystallogr. 42 (2009) 347–353, https://doi.org/10.1107/S0021889809002222.
[29] G. Beaucage, Approximations leading to a unified exponential power-law approach to small-angle scattering, J. Appl. Crystallogr. 28 (1995) 717–728, https://doi.org/10.1107/S0021889895005292.
[30] W.P. Cox, E.H. Merz, Correlation of dynamic and steady flow viscosities, J. Polym. Sci. 28 (1958) 619–622, https://doi.org/10.1002/pol.1958.1202811812.
[31] RCoreTeam, A Language and Environment for Statistical Computing, 2023.
[32] P. Schiener, K.D. Black, M.S. Stanley, D.H. Green, The seasonal variation in the chemical composition of the kelp species laminaria digitata, laminaria hyperborea, saccharina latissima and alaria esculenta, J. Appl. Phycol. 27 (2015) 363–373, https://doi.org/10.1007/s10811-014-0327-1.
[33] J.V. Vilg, G.M. Nylund, T. Werner, L. Qvirist, J.J. Mayers, H. Pavia, I. Undeland, E. Albers, Seasonal and spatial variation in biochemical composition of saccharina latissima during a potential harvesting season for western Sweden, Bot. Mar. 58 (2015) 435–447, https://doi.org/10.1515/bot-2015-0034.
[34] M.M. Nielsen, D. Manns, M. D'Este, D. Krause-Jensen, M.B. Rasmussen, M. M. Larsen, M. Alvarado-Morales, I. Angelidaki, A. Bruhn, Variation in biochemical composition of saccharina latissima and laminaria digitata along an estuarine salinity gradient in inner danish waters, Algal Research-Biomass Biofuels and Bioproducts 13 (2016) 235–245, https://doi.org/10.1016/j.algal.2015.12.003.
[35] C. Dawczynski, R. Schubert, G. Jahreis, Amino acids, fatty acids, and dietary fibre in edible seaweed products, Food Chem. 103 (2007) 891–899, https://doi.org/10.1016/j.foodchem.2006.09.041.
[36] H.O. Mohammed, M.N. O'Grady, M.G. O'Sullivan, R.M. Hamill, K.N. Kilcawley, J. P. Kerry, An assessment of selected nutritional, bioactive, thermal and technological properties of brown and red irish seaweed species, Foods 10 (2021) 2784, https://doi.org/10.3390/foods10112784.
[37] M.B. Samarasinghe, M.E. van der Heide, M.R. Weisbjerg, J. Sehested, J.J. Sloth, A. Bruhn, M. Vestergaard, J.N. V., L.E. Hernandez-Castellano, A descriptive chemical analysis of seaweeds, Ulva sp., saccharina latissima and ascophyllum nodosum harvested from danish and icelandic waters, Anim. Feed Sci. Technol. 278 (2021) 115005, https://doi.org/10.1016/j.anifeedsci.2021.115005.
[38] B. Li, F. Lu, X. Wei, R. Zhao, Fucoidan: structure and bioactivity, Molecules 13 (2008) 1671–1695, https://doi.org/10.3390/molecules13081671.
[39] L. Allahgholi, R.R.R. Sardari, S. Hakvag, K.Z.G. Ara, T. Kristjansdottir, I.M. Aasen, O.H. Fridjonsson, T. Brautaset, G.O. Hreggvidsson, E.N. Karlsson, Composition analysis and minimal treatments to solubilize polysaccharides from the brown seaweed laminaria digitata for microbial growth of thermophiles, J. Appl. Phycol. 32 (2020) 1933–1947, https://doi.org/10.1007/s10811-020-02103-6.
[40] B.H.J. Yap, G.J. Dumsday, P.J. Scales, G.J.O. Martin, Energy evaluation of algal cell disruption by high pressure homogenisation, Bioresour. Technol. 184 (2015) 280–285. URL: https://doi.org/10.1016/j.biortech.2014.11.049.
[41] H. Bojorges, A. Martinez-Abad, M. Martinez-Sanz, M.D. Rodrigo, F. Vilaplana, A. Lopez-Rubio, M.J. Fabra, Structural and functional properties of alginate obtained by means of high hydrostatic pressure-assisted extraction, Carbohydr. Polym. 299 (2023) 120175, https://doi.org/10.1016/j.carbpol.2022.120175.
[42] G. Kavanagh, S. Ross-Murphy, Rheological characterisation of polymer gels, Prog. Polym. Sci. 23 (1998) 533–562, https://doi.org/10.1016/S0079-6700(97)00047-6.
[43] A.H. Clark, S. Ross-Murphy, Structural and mechanical properties of biopolymer gels, in: Biopolymers, Springer Berlin Heidelberg, Berlin, Heidelberg, 1987, pp. 57–192.